

Non-parametric ordinal regression under a monotonicity constraint

Olli Saarela^{*1}, Christian Rohrbeck², and Elja Arjas^{3,4}

¹Dalla Lana School of Public Health, University of Toronto

²Department of Mathematical Sciences, University of Bath

³University of Helsinki

⁴University of Oslo

Abstract

Compared to the nominal scale, ordinal scale for a categorical outcome variable has the property of making a monotonicity assumption for the covariate effects meaningful. This assumption is encoded in the commonly used proportional odds model, but there it is combined with other parametric assumptions such as linearity and additivity. Herein, we consider models where monotonicity is used as the only modeling assumption when modeling the effects of covariates on the cumulative probabilities of ordered outcome categories. We are not aware of other non-parametric multivariable monotonic ordinal models for inference purposes. We generalize our previously proposed Bayesian monotonic multivariable regression model to ordinal outcomes, and propose an estimation procedure based on reversible jump Markov chain Monte Carlo. The model is based on a marked point process construction, which allows it to approximate arbitrary monotonic regression function shapes, and has a built-in covariate selection property. We study the performance of the proposed approach through extensive simulation studies, and demonstrate its practical application in two real data examples.

Keywords: Monotonic regression; Non-parametric Bayesian regression; Ordinal regression; Proportional odds models.

*Correspondence to: Olli Saarela, Dalla Lana School of Public Health, 155 College Street, Toronto, Ontario M5T 3M7, Canada. Email: olli.saarela@utoronto.ca

1 Introduction

Ordinal data consist of categorical variables measured on a scale that has a natural ordering, but where there may not exist well-defined distances between the categories or where such distances have been left unspecified (Agresti, 2010). In regression models for ordinal data, the response variable $Y \in \{A_1, \dots, A_K\}$, where $K \geq 1$ and $A_1 \prec A_2 \prec \dots \prec A_K$, is a linear order of the possible response levels, while the predictors $\mathbf{x} = (x_1, \dots, x_p)$ can be of any scale. In typical applications, such as when filling in questionnaires for political opinion polls, the categories could vary from A_1 signifying strong disagreement to A_5 representing strong agreement. Similarly, in customer rating of hotels or restaurants, the categories could be grades from a single star (*) to five stars (*****). Data of this type are commonly treated by applying the Likert scale with numerical values from 1 to 5, in spite of that it may be difficult to argue, for example, that the difference between grades 1 and 2 should be qualitatively similar to the difference between 4 and 5.

Compared to nominal scale, an important property of ordinal scale outcome variables is that for them the definition of monotonicity w.r.t. the covariates is meaningful. This property was formulated by Lehmann (1966) as positive regression dependency between variables Y and X , meaning that the probabilities $P(Y \leq y \mid X = x)$ are non-decreasing in x (Agresti, 2010, p. 43). In the present context, the corresponding property can be defined as

$$\mathbf{x}_1 \leq \mathbf{x}_2 \Rightarrow S(k \mid \mathbf{x}_1) \leq S(k \mid \mathbf{x}_2), \quad (1)$$

where $S(k \mid \mathbf{x})$ is the “survival function” $S(k \mid \mathbf{x}) = P(Y \succeq A_k \mid \mathbf{x})$, $k = 1, \dots, K$.

Parametric forms of ordinal regression models have been considered widely in the statistical literature, with textbook-level treatments given, for example, by Congdon (2005), Johnson and Albert (1999), Agresti (2010) and Harrell Jr (2015), and methodological reviews provided by Ananth and Kleinbaum (1997) and Lall et al. (2002). By far the most popular model is the ordinal logistic, or proportional odds model, attributed to McCullagh (1980). The proportionality property is formulated by writing, for $k = 2, \dots, K$, the log-odds in the form of the linear expression

$$\log \left\{ \frac{S(k \mid \mathbf{x})}{1 - S(k \mid \mathbf{x})} \right\} = \text{logit} \{S(k \mid \mathbf{x})\} = \alpha_k + \beta' \mathbf{x} \quad (2)$$

or, equivalently,

$$S(k | \mathbf{x}) = \text{expit}(\alpha_k + \beta' \mathbf{x}) = \frac{1}{1 + \exp\{-(\alpha_k + \beta' \mathbf{x})\}}.$$

Since the values of the probabilities $S(k | \mathbf{x})$ decrease in k for fixed \mathbf{x} , we have $\alpha_2 > \alpha_3 > \dots > \alpha_K$. The attribute “proportional odds” stems from that, in (2), the same regression coefficients β are used for all $k = 2, \dots, K$. Thus, in a comparison between probabilities $S(k | \mathbf{x})$ and $S(\ell | \mathbf{x})$, when both are based on a common covariate value \mathbf{x} , the resulting odds ratio $\exp\{\alpha_k - \alpha_\ell\}$ is constant in \mathbf{x} . On the other hand, when fixing the category level k but considering two covariate values \mathbf{x}_1 and \mathbf{x}_2 , the odds ratio becomes $\exp\{\beta'(\mathbf{x}_1 - \mathbf{x}_2)\}$. Since this expression does not depend on k , it follows that, if the regression coefficients β_j are non-negative, then (1) holds for all $k = 1, \dots, K$. Expressed in words, increasing the values of the covariates \mathbf{x} has the effect of stochastically increasing the outcome variable Y with respect to the ordering \prec . The conclusion on the right of (1) can be denoted compactly by $Y | \mathbf{x}_1 \prec_{\text{st}} Y | \mathbf{x}_2$. It is obvious that if $\beta_j < 0$ for some $j = 1, \dots, p$, the conclusion still holds if $\beta'(\mathbf{x}_1 - \mathbf{x}_2) > 0$. Espinosa and Hennig (2019) recently extended the proportional odds formulation to include ordinal predictors, entered into the linear predictor through dummy variables, with monotonicity constraints for the respective regression coefficients.

Several authors have noted that the constant proportionality assumption of model (2) can in practice be unduly restrictive in order to provide an adequate description for empirical data. Statistical tests for assessing the validity of the proportionality property have been derived, either by assessing the general goodness-of-fit of the model (Ashby et al., 1986) or by comparing it to models in which this property has been relaxed (Brant, 1990). In the non-proportional odds (NPO) model, the regression coefficients β_j are allowed to vary with category level A_k , while in the partial proportional odds (PPO) model, such variation is possible in a subset of all levels (e.g. Peterson and Harrell Jr, 1990; Bender and Grouven, 1998; Tutz and Scholz, 2003). The key challenge in fitting such models is to ensure that the stochastic ordering conditions hold for any chosen explanatory variables (McKinley et al., 2015). Additional variants consist of cumulative link models (Agresti, 2003), where link function differs from the logit, common choices being probit, log-log and complementary log-log.

Bayesian formulations of the proportional odds model are commonly based on

introducing a continuous-valued latent variable ε , such that $P(Y = A_k | \mathbf{X}) = P(\alpha_k - \beta' \mathbf{x} < \varepsilon < \alpha_{k+1} - \beta' \mathbf{x})$. Assuming ε to be standard logistic or standard normally distributed would give logit and probit models, respectively; in the latter, computational efficiency has been enhanced by applying data augmentation for the latent variable (e.g. Albert and Chib, 1993; Johnson and Albert, 1999). The Bayesian formulation has also enabled further non-parametric extensions of the original model, as in Chib and Greenberg (2010), Bao and Hanson (2015) and DeYoreo and Kottas (2018).

The practical goal of the statistical literature briefly reviewed above has been in attempts to explain and to quantify the effects which variations in the covariate values have on the outcome of interest. Ordinal regression has been studied extensively also in the machine learning literature, albeit with a somewhat different focus, from the perspective of successful automated classification. The interpretability of the model structure, or of its parameters, has then had a smaller or no role. A good survey is provided by Gutierrez et al. (2015).

In the present paper, our interest is in non-parametric estimation under the monotonicity constraint (1), in a form that would not impose additional parametric or distributional assumptions or make use of continuous latent variable formulations. Our goal is then to demonstrate that, by Bayesian ‘borrowing of strength’ from neighbouring model structures, the constraint would in itself impose a sufficient degree of regularity for successful estimation of the regression functions.

The corresponding non-parametric optimization problem of minimizing the sum of squared prediction errors, under monotonicity constraints, is known as isotonic regression (Barlow and Brunk, 1972). Kotlowski and Slowinski (2012) considered an extension of this for the classification of an ordinal response variable under (1). Their approach directly minimized a linear loss function of the difference between the actual and predicted categories. Stout (2015) proposed an algorithm for multivariable isotonic regression. However, we are not aware of non-parametric and monotonic ordinal regression approaches for inferential purposes in the above sense. To achieve this, we extend in this work the Bayesian monotonic regression approach of Saarela and Arjas (2011) for ordered multi-category responses.

We note that there are other Bayesian monotonic regression methods that could potentially be extended to ordinal responses, such as the projection-based approach of Lin and Dunson (2014) or the tree-based one of Chipman et al. (2016). We chose

the approach of Saarela and Arjas (2011) for the extension since it can approximate arbitrary monotonic regression functions, it incorporates a useful covariate selection feature, handles both continuous and ordinal predictors, and can be naturally adapted to multiple ordered regression surfaces without additional structural assumptions. The formulation is based on marked point processes, and the estimation procedure is based on reversible jump Markov chain Monte Carlo (Green, 1995).

The paper is structured as follows: in Section 2 we formulate the proposed model and MCMC algorithm for estimation. In Section 3 we present results of simulation studies for the properties of the method, and in Section 4 we demonstrate its use in real data. We conclude with a discussion in Section 5.

2 Model and estimation method

2.1 Model construction

The notation builds on that used by Saarela and Arjas (2011), where

A probability model for y is defined as $p(y | \lambda(x_1, \dots, x_p), \theta)$. Here $\lambda : \mathbb{R}^p \rightarrow A$ is a single realization of a random monotonic function of the covariates $\mathbf{x} = (x_1, \dots, x_p)$, while θ includes possible other parameters. $A \subseteq \mathbb{R}$ is the set where the regression function is defined.

To extend such a model to ordinal responses, we introduce functions $S(k | \mathbf{x}; \lambda_k) = P(Y \succeq A_k | \mathbf{x}; \lambda_k)$, $k = 2, \dots, K$, where $\lambda_k : \mathbb{R}^p \rightarrow A$ is a realization of a random regression function mapping the covariate space to probabilities of the outcome variable categories, possibly on a link function scale. We formulate the model first without a link function, in which case we have simply that $A = [0, 1]$ and $S(k | \mathbf{x}; \lambda_k) = \lambda_k(\mathbf{x})$. The likelihood for the λ_k s, given the observed data $\mathcal{D}_N = \{(\mathbf{x}_n, Y_n); 1 \leq n \leq N\}$, is then

$$L(\lambda_1, \dots, \lambda_K; \mathcal{D}_N) = \prod_{n=1}^N \prod_{k=1}^K [S(k | \mathbf{x}_n; \lambda_k) - S(k+1 | \mathbf{x}_n; \lambda_{k+1})]^{\mathbf{1}_{\{Y_n = A_k\}}},$$

where $S(1 | \mathbf{x}) = 1$ and $S(K+1 | \mathbf{x}) = 0$ by definition. Our interest is in the posterior distribution of the λ_k s under a suitably flexible prior specification.

The key monotonicity property postulated is that, for $1 \leq k \leq K$, the realizations $S(k | \mathbf{x}; \lambda_k)$ are non-increasing in \mathbf{x} , i.e., $S(k | \mathbf{x}_1; \lambda_k) \leq S(k | \mathbf{x}_2; \lambda_k)$ whenever $\mathbf{x}_1 \leq \mathbf{x}_2$. In addition, being ‘survival’ probabilities of ordered outcome categories, they are restricted by $S(k | \mathbf{x}; \lambda_k) \geq S(\ell | \mathbf{x}; \lambda_k)$, where $1 \leq k < \ell \leq K$, for all \mathbf{x} . The same ordering constraints apply obviously to the λ_k s also if specified on the scale of a monotonic link function.

As the prior specification for the regression functions λ_k , we use a marked point process construction similar to Saarela and Arjas (2011) and Rohrbeck et al. (2018). For simplicity, we assume that each covariate has been scaled to the interval $[0, 1]$, as the covariates’ scales do not carry information in non-parametric regression. In the construction, the pair $(\boldsymbol{\xi}_{ij}, \delta_{ij})$ represents the location and the mark of a point $j = 1, \dots, n(\Delta_i)$ originating from a spatial point process $\Delta_i = \{(\boldsymbol{\xi}_{ij}, \delta_{ij})\} \subset X_i \times A$, where $i \in \{1, \dots, s\}$ and $A = [0, 1]$ if no link function is used. Although in principle we could take $s = 1$ to specify only a single spatial point process in the space $X_1 = [0, 1]^p$ of all covariates, in order to allow the construction to have the ability to perform covariate selection, we also define the point processes in the $s = 2^p - 1$ lower-dimensional subspaces determined by the non-empty subsets of $\{1, \dots, p\}$. For example, with $p = 2$, we would take $s = 3$ with $X_1 = X_2 = [0, 1]$ and $X_3 = [0, 1]^2$. To be able to place the points in the common covariate space $[0, 1]^p$, we introduce completed versions $\tilde{\boldsymbol{\xi}}_{ij} \in [0, 1]^p$ where the ‘missing’ coordinates are set to zero. In the example then $\tilde{\boldsymbol{\xi}}_{1j} = (\tilde{\xi}_{1j1}, 0)$, $\tilde{\boldsymbol{\xi}}_{2j} = (0, \tilde{\xi}_{2j2})$ and $\tilde{\boldsymbol{\xi}}_{3j} = (\tilde{\xi}_{3j1}, \tilde{\xi}_{3j2}) \in [0, 1]^2$; see also Figure 2 in Rohrbeck et al. (2018). This allows for automatic reduction of the dimensionality of the problem in case some of the covariates are not relevant to the problem, by allowing the model fit to use only a subset of the available point processes. Each point process is a priori taken to be a homogeneous Poisson point process with rate $\rho_i \sim \text{Gamma}(a, b)$. Conditionally on the current point configuration, the marks are assumed a priori jointly uniformly distributed in the space restricted by the ordering constraints. Thus, the only specific prior information is expressed in the monotonicity assumption.

When extending the construction to ordinal regression, we take $\Delta_i = \{(\boldsymbol{\xi}_{ij}, \boldsymbol{\delta}_{ij})\} \subset X_i \times [0, 1]^{K-1}$, with each mark now a random vector $\boldsymbol{\delta}_{ij} = (\delta_{ij1}, \dots, \delta_{ijK})$, where $\delta_{ij1} \leq \delta_{ij2} \leq \dots \leq \delta_{ijK}$, with $\delta_{ij1} = 1$ by definition, and δ_{ijk} reflecting the value of the regression function $\lambda_k(\mathbf{x})$ at point $\mathbf{x} = \tilde{\boldsymbol{\xi}}_{ij}$, i.e., $\lambda_k(\tilde{\boldsymbol{\xi}}_{ij}) = \delta_{ijk}$. In addition, a fixed point $(\tilde{\boldsymbol{\xi}}_{01}, \boldsymbol{\delta}_{01})$ with mark $\boldsymbol{\delta}_{01} = (\delta_{011} = 1, \delta_{012}, \dots, \delta_{01K})$ is placed at the origin. It is

obvious that the value of the regression function $\lambda_k(\mathbf{x})$ at point \mathbf{x} is constrained to lie in the interval $[\max\{\delta_{ijk} : \tilde{\boldsymbol{\xi}}_{ij} \preceq \mathbf{x}\}, \min\{\delta_{ijk} : \tilde{\boldsymbol{\xi}}_{ij} \succeq \mathbf{x}\}]$. In principle there would be many alternative ways to define the regression function realizations with these properties, but for computational simplicity we choose $\lambda_k(\mathbf{x}) = \max\{\delta_{ijk} : \tilde{\boldsymbol{\xi}}_{ij} \preceq \mathbf{x}\}$, $1 \leq k \leq K$.

We note that in the proposed construction, the locations of the support points $\tilde{\boldsymbol{\xi}}_{ij}$ are shared between the $K - 1$ regression functions, with separate ordered levels. Alternatively it would have been possible to define separate spatial point processes for the different functions, but the proposed structure is more parsimonious, while still allowing the levels δ_{ijk} to move freely within the ordering constraints.

2.2 Semi-parametric models

While the assumption of monotonicity provides structure to the problem, estimation of non-parametric models involving a large number of covariates eventually becomes difficult due to the curse of dimensionality. To be able to incorporate more covariates, and use the non-parametric monotonic structure where it is most needed, we also introduce a semi-parametric version of the model. We allow the functions $S(k | \mathbf{x}, \mathbf{z}; \lambda_k, \theta)$ to depend on additional covariates $\mathbf{z} = (z_1, \dots, z_q)$ and parameters θ , and using the logit link as in (2), the regression functions λ_k take the role of the level-specific intercept terms in (2):

$$\log \left(\frac{S(k | \mathbf{x}, \mathbf{z}; \lambda_k, \theta)}{1 - S(k | \mathbf{x}, \mathbf{z}; \lambda_k, \theta)} \right) = \lambda_k(\mathbf{x}) + \sum_{j=1}^q \beta_j z_j, \quad (3)$$

where $\theta = (\beta_1, \dots, \beta_q)$. The prior specification for λ_k s is otherwise the same as in Section 2.1, but instead of the interval $[0, 1]$, these functions map to some a priori chosen interval $A \subset (-\infty, \infty)$. With a view to the data analysis example of Section 4, we also note that we can deal with clustered data by introducing random effects into the linear predictor, such as in

$$\log \left(\frac{S(k | \mathbf{x}, \mathbf{z}, c; \lambda_k, \theta)}{1 - S(k | \mathbf{x}, \mathbf{z}, c; \lambda_k, \theta)} \right) = \lambda_k(\mathbf{x}) + \sum_{j=1}^q \beta_j z_j + \gamma_c,$$

where $\theta = (\beta_1, \dots, \beta_q, \gamma_1, \dots, \gamma_C)$ and $c \in \{1, \dots, C\}$ is a variable indicating cluster membership, and the cluster effects ('random intercepts') are a priori independent

and identically distributed draws from a distribution such as $\gamma_c \sim N(0, \tau^2)$.

2.3 Markov chain Monte Carlo algorithm

2.3.1 Updating moves

We use MCMC to propose local modifications to the current regression function realizations, thereby exploring the space of possible versions of such functions. Here the postulated ordering constraints provide information for the construction of reasonable proposals. We use prior proposals for updating the function levels, which leads to simple forms for the Metropolis-Hastings (M-H) ratios. To demonstrate this, we note that given the current point configuration with a total of $M = (K-1)(1 + \sum_{i=1}^s n(\Delta_i))$ marks and denoting the vectors of the marks by $\boldsymbol{\delta}_i = (\boldsymbol{\delta}_{i1}, \boldsymbol{\delta}_{i2}, \dots, \boldsymbol{\delta}_{in(\Delta_i)})$, $i \in \{1, \dots, s\}$, and $\boldsymbol{\delta}_0 = (\boldsymbol{\delta}_{01})$ for the fixed point at the origin, the joint prior density of all the marks $\boldsymbol{\delta} = (\boldsymbol{\delta}_0, \boldsymbol{\delta}_1, \dots, \boldsymbol{\delta}_s)$ has the expression

$$f(\boldsymbol{\delta}) = \frac{M!}{M^*} \left(\frac{1}{|A|} \right)^M.$$

Here $M!$ is the total number of permutations, and M^* is the number of these permutations that satisfy the ordering constraints depending in part on the location of the points. All the resulting full conditional distributions are also uniform; to see this, we can write, for example, the conditional density for the mark vector of a single point, given all others, as

$$f(\boldsymbol{\delta}_{ij} \mid \boldsymbol{\delta}_{-ij}) = \frac{f(\boldsymbol{\delta})}{f(\boldsymbol{\delta}_{-ij})} = \frac{M!}{M^*} \left(\frac{1}{|A|} \right)^M \frac{1}{f(\boldsymbol{\delta}_{-ij})}$$

for values $\boldsymbol{\delta}_{ij}$ satisfying the ordering constraints and zero otherwise. Here the marginal density in the denominator simply normalizes the uniform density in the numerator. The marginal densities are generally non-uniform, but need not be known as the conditional priors can be simulated from and cancel out from the M-H ratios without having to evaluate the normalizing constant. In practice this can proceed by sampling uniformly distributed mark vectors until one satisfying the ordering constraints is drawn.

Some of the proposals change the dimension of the parameter space, requiring reversible jump type updating moves for dimension matching (Green, 1995). The list

of the proposed moves in the algorithm and the corresponding M-H ratios are listed as follows:

1. Birth step. A point process i for the proposal is selected randomly. A location for a new point in point process i is selected uniformly from X_i . Given the partial ordering constraints imposed by the new location and the currently existing points, the function levels are drawn from the uniform distribution in the space where the ordering constraints are satisfied. The proposed new regression surfaces $\lambda_1^*, \dots, \lambda_K^*$ are accepted with probability

$$\min \left\{ 1, \frac{L(\lambda_1^*, \dots, \lambda_K^*; \mathcal{D}_N) \rho_i |X_i|}{L(\lambda_1, \dots, \lambda_K; \mathcal{D}_N) (n(\Delta_i) + 1)} \right\}.$$

2. Death step. A point process i for the proposal is selected randomly. One of the currently existing points is randomly selected as a candidate for removal, with the regression surfaces modified accordingly. The removal is accepted with probability

$$\min \left\{ 1, \frac{L(\lambda_1^*, \dots, \lambda_K^*; \mathcal{D}_N) n(\Delta_i)}{L(\lambda_1, \dots, \lambda_K; \mathcal{D}_N) \rho_i |X_i|} \right\}.$$

3. Combined death-birth step. One of the point processes i is randomly selected for removal and another one, say i' , is selected as candidate for having a new point. The previous death and birth steps are then attempted together, and this is accepted with probability

$$\min \left\{ 1, \frac{L(\lambda_1^*, \dots, \lambda_K^*; \mathcal{D}_N) \rho_{i'} |X_{i'}| n(\Delta_i)}{L(\lambda_1, \dots, \lambda_K; \mathcal{D}_N) \rho_i |X_i| (n(\Delta_{i'}) + 1)} \right\}.$$

4. Position change step. An existing location $\tilde{\xi}_{ij}$ is randomly selected for a move, and a new location is drawn uniformly from $\prod_{k=1}^p [\max\{\tilde{\xi}_{rs}^k : \tilde{\xi}_{rs}^k \leq \tilde{\xi}_{ij}^k, 0\}, \min\{\tilde{\xi}_{rs}^k : \tilde{\xi}_{rs}^k \geq \tilde{\xi}_{ij}^k, 1\}]$, where $(r, s) \neq (i, j)$. This will not change the position of the point to be beyond its closest neighbors, so the ordering constraints are not violated. The move is accepted with probability involving only the likelihood ratio.

5. Joint level change step. An existing location $\tilde{\xi}_{ij}$ is randomly selected for an update. New values for the levels $\boldsymbol{\delta}_{ij} = (\delta_{ij1}, \dots, \delta_{ijK})$ are drawn from the

uniform distribution in the space restricted by the current ordering constraints. The proposal is accepted with probability involving only the likelihood ratio.

6. Single level change step. An existing location $\tilde{\xi}_{ij}$ and one level δ_{ijk} are randomly selected for an update. A new value for the level is drawn randomly from the uniform distribution on the interval restricted by the current ordering constraints. The proposal is accepted with probability involving only the likelihood ratio.

In addition to the above Metropolis-Hasting moves, and conditionally on the current point configuration, the Poisson intensities are updated from the conjugate posteriors $\rho_i \sim \text{Gamma}(a + n(\Delta_i), b + |X_i|)$. For efficient computation, the MCMC algorithm was implemented in C programming language, called from R statistical environment (R Core Team, 2020) through the `.C` interface.

2.3.2 Conditional prior to counter “spiking” behaviour

The classical isotonic regression is reported to produce inconsistent estimates at the boundaries of the support of the data; this phenomenon was called the “spiking” problem by Wu et al. (2015), who proposed penalized estimation as a solution. The unstable behaviour at the boundaries can be an issue also for the proposed Bayesian implementation as it does not impose any smoothness on the regression function realizations. To counter such behaviour close to the origin, where the function levels are not constrained from below by other support points, we also experimented with a modified prior, where the function levels δ_{01k} , $k \in \{2, \dots, K\}$, at the origin have the conditional prior specification $\delta_{01k} \mid \boldsymbol{\delta}_{-01k} \sim \text{Beta}(1 + \min(\sum_{i=1}^s n(\Delta_i), d), 1) \times (\delta_{\max} - \delta_{\min}) + \delta_{\min}$, that is, a left-skewed Beta distribution scaled to the interval $[\delta_{\min}, \delta_{\max}]$ determined by the partial ordering constraints imposed by the current point configuration. This prior allows borrowing information from the regression surface levels near the origin; the updating moves are as in step 6 above, using prior proposals accepted with the likelihood ratio. Here the choice of the constant d determines the level of penalization, with $d = 0$ returning the previous non-informative uniform prior.

Some results from applying this alternative prior, in the context of the discontinuous survival functions of Section 3.1, are described in Section S1.4 of the online Supplementary Material.

3 Numerical Examples

We apply our approach to the two ordinal regression models described in Section 2. In Section 3.1, the survival functions are defined directly in terms of non-parametrically specified monotonic functions, that is, $S(k | \mathbf{x}; \lambda_k) = \lambda_k(\mathbf{x})$, $k = 1, \dots, K$. Section 3.2 considers the semi-parametric model structure defined in (3). Across all studies, the number of categories was set to $K = 5$, corresponding to the Likert scale with values from 1 to 5. The functions $\lambda_1, \dots, \lambda_K$ were defined on the unit square, i.e., $\lambda_k : [0, 1]^2 \rightarrow \mathbb{R}$, $k = 1, \dots, 5$.

In the experiments, data sets of size $N = 1000$ and $N = 5000$ were generated, with values \mathbf{x} sampled independently from the uniform distribution on the unit square. The samples of size $N = 1000$ were subsets of those of size $N = 5000$, and 20 independent repetitions of this procedure were performed. Independent gamma priors were specified for the point process intensities, $\rho_i \sim \text{Gamma}(0.1, 0.1)$, $i = 1, \dots, s$. Approximate samples from the posterior were obtained by running the Markov chain Monte Carlo sampler, described in Section 2, for 500,000 iterations after a burn-in period of 100,000, and then saving every 50th state of the chain. Trace plots illustrating convergence and mixing of the functional levels $\lambda_k(\mathbf{x})$ at some of the simulated values of \mathbf{x} are provided in Section S1.2 of the Supplementary Material.

To measure performance, we consider the probabilities $\mathbb{P}(k | \mathbf{x}_n)$ instead of the monotonic functions $\lambda_k(\mathbf{x}_n)$, $n = 1, \dots, N$. Let $\hat{p}(k | \mathbf{x}_n)$ denote the posterior mean probability of category k at the covariate value \mathbf{x}_n , computed as the Monte Carlo average of the corresponding sampled values. Then, for each category, we calculate the mean absolute difference of $\mathbb{P}(k | \mathbf{x}_n)$ and $\hat{p}(k | \mathbf{x}_n)$ across the data points with $y_n = k$. Formally, for $\mathcal{D}_k = \{n \in \{1, \dots, N\} : y_n = k\}$ and L posterior samples, the performance measure for category k is defined as

$$\text{MAE}(k) = \frac{1}{|\mathcal{D}_k|L} \sum_{n \in \mathcal{D}_k} \sum_{\ell=1}^L |\hat{p}^{(\ell)}(y_n | \mathbf{x}_n) - \mathbb{P}(y_n | \mathbf{x}_n)|, \quad (4)$$

where $\hat{p}^{(\ell)}$ denotes the estimated probability based on the ℓ -th sample.

Another aspect we wish to investigate is the ability of our approach to estimate the survival function $S(k | \cdot)$, $k = 1, \dots, K$ across the covariate space, rather than just at the points \mathbf{x}_n with $y_n = k$. Again, we focus on the observed covariate values, $\mathbf{x}_1, \dots, \mathbf{x}_N$, but now consider the vector $[\mathbb{P}(1 | \mathbf{x}_n), \dots, \mathbb{P}(K | \mathbf{x}_n)]$ instead of $\mathbb{P}(y_n | \mathbf{x}_n)$.

Table 1: Error measures $\text{MAE}(k) \times 10^2$ and $\text{MAE} \times 10^2$, with standard deviations $\times 10^2$, computed from 20 sets of simulated data from the models in Figure 1, for $n = 1000$ and $n = 5000$.

Functions	N	MAE(1)	MAE(2)	MAE(3)	MAE(4)	MAE(5)	MAE
Linear	1000	3.8 (1.1)	2.1 (0.6)	1.8 (0.5)	2.2 (0.6)	3.0 (0.7)	4.1 (0.2)
	5000	2.2 (0.4)	1.3 (0.3)	1.3 (0.3)	1.4 (0.3)	2.0 (0.3)	2.6 (0.1)
Cont.	1000	4.3 (0.8)	2.9 (0.7)	2.3 (0.6)	2.1 (0.6)	3.0 (0.8)	4.6 (0.2)
	5000	2.9 (0.4)	1.6 (0.3)	1.5 (0.4)	1.4 (0.4)	1.8 (0.4)	2.9 (0.2)
Discont.	1000	4.4 (0.9)	3.7 (0.4)	4.2 (0.6)	4.8 (0.5)	3.7 (0.7)	4.7 (0.3)
	5000	2.7 (0.4)	2.2 (0.3)	2.1 (0.4)	2.5 (0.3)	2.1 (0.4)	2.7 (0.2)

The overall model fit is then measured by

$$\text{MAE} = \frac{1}{NKL} \sum_{n=1}^N \sum_{k=1}^K \sum_{\ell=1}^L |\hat{p}^{(\ell)}(k | \mathbf{x}_n) - \mathbb{P}(k | \mathbf{x}_n)|.$$

3.1 Non-parametric model structures

Figure 1 shows three sets of survival functions $S(2 | \mathbf{x}), \dots, S(5 | \mathbf{x})$, which we use here as illustrations of the method; $S(1 | \mathbf{x}) = 1$ and is therefore omitted from the figure. The exact definitions of these functions are provided in Section S1.1 of the online supplementary material. In our first example, the functions $\lambda_2, \dots, \lambda_5$ are linear, with λ_2 and λ_5 having identical slopes, and similarly for λ_3 and λ_4 . In the second example, the survival functions are constant when one of two predictors has a small value, and increase continuously otherwise. In the third example the survival functions are discontinuous, with each function $S(2 | \mathbf{x}), \dots, S(5 | \mathbf{x})$ having a different set of discontinuity points. The proportions of data points in the different categories varied: in the first example, there were approximately similar numbers of data points in each category; in the second, the largest number of points were in category 1, followed by category 5; while in the third example, category 5 had the largest number of data points.

The posterior estimates in Figure 2 show that our methodology correctly identifies the overall structure of the underlying model functions in Figure 1; more plots illustrating the uncertainty of the model estimates and general model fit are provided in S1.3 of the online Supplementary Material. From Table 1 we can see that the

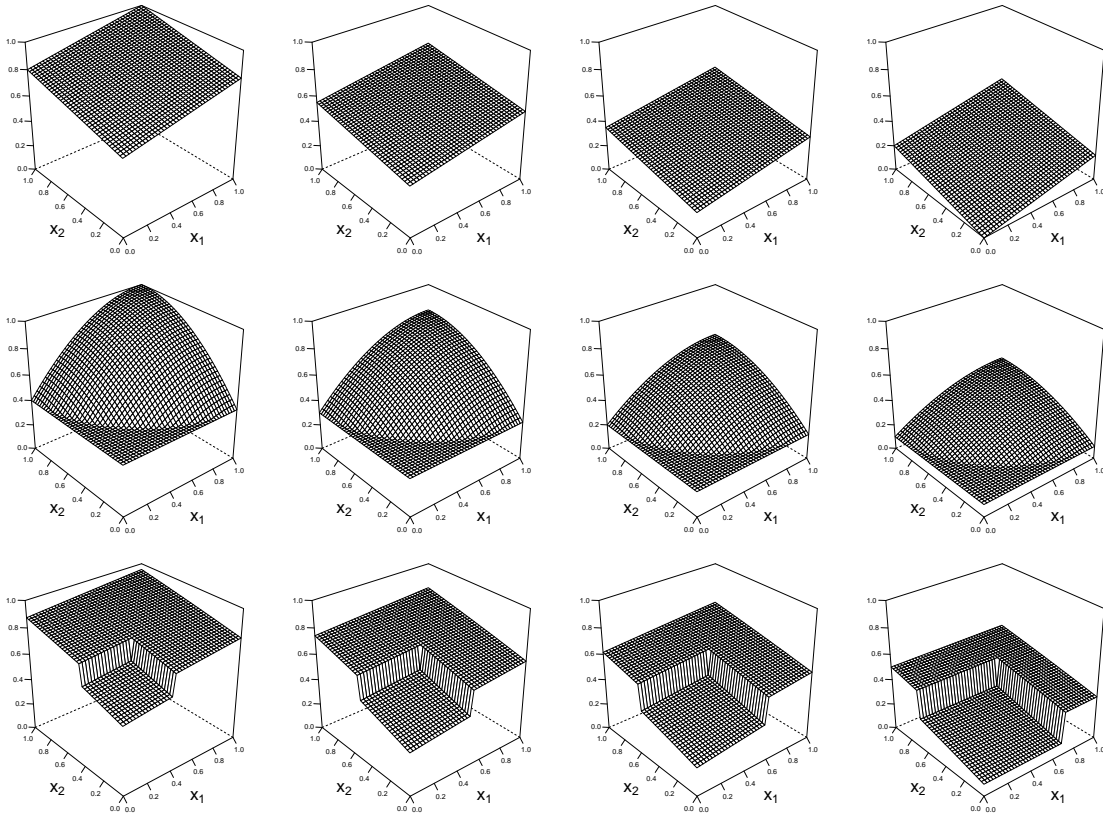


Figure 1: Graphical displays of the survival functions $S(2 | \cdot), \dots, S(5 | \cdot)$ (left to right) considered in Section 3.1: linear functions (top), continuous (middle), and discontinuous (bottom).

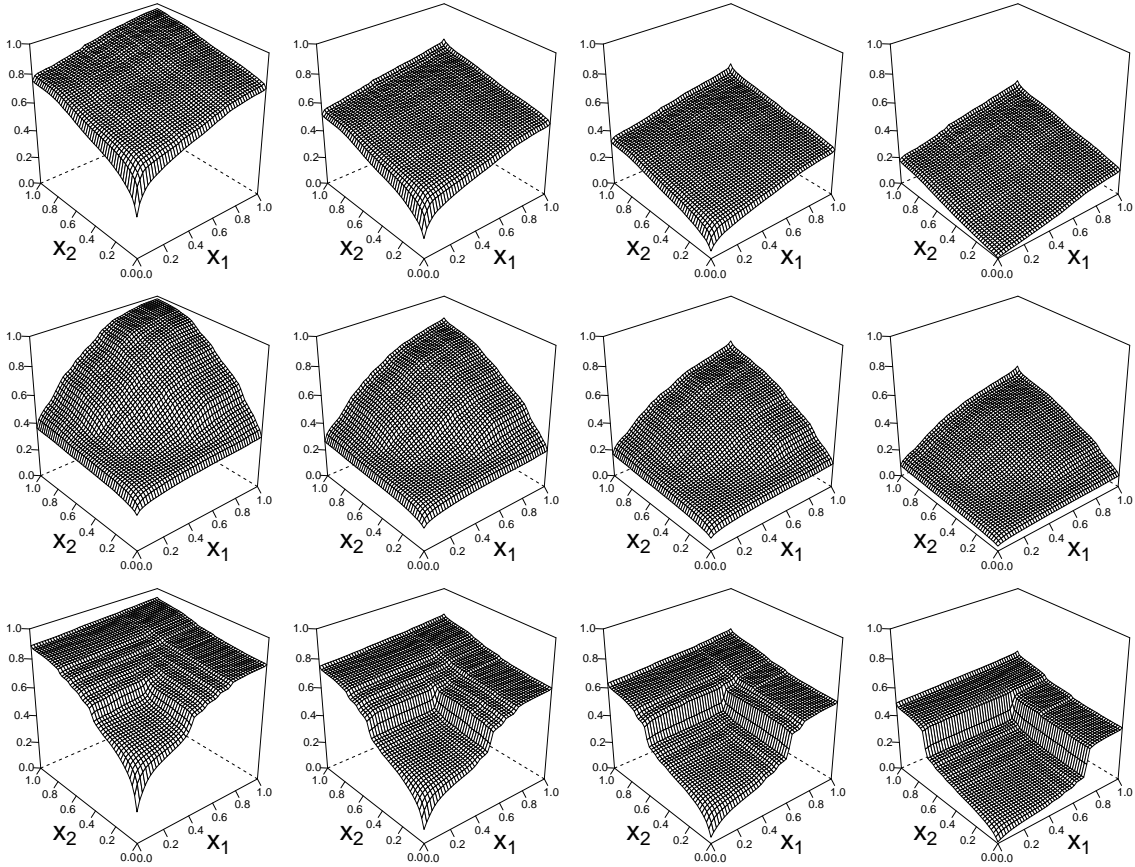


Figure 2: Graphical displays of the posterior mean estimates of the survival functions $S(2 | \cdot), \dots, S(5 | \cdot)$ in Section 3.1, averaged over results from 20 simulated data sets of size $N = 5000$: linear (top), continuous (middle), and discontinuous (bottom).

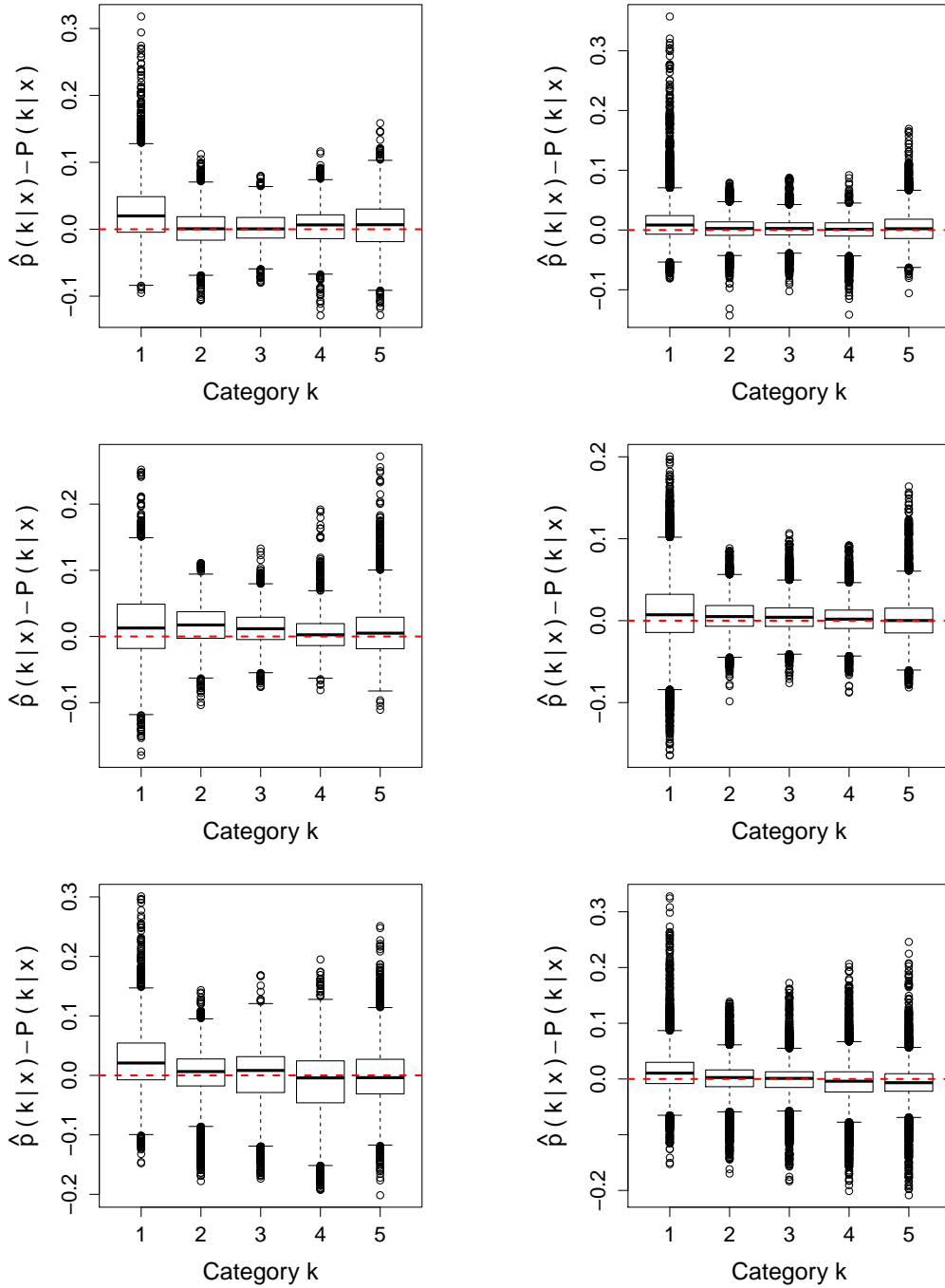


Figure 3: Boxplots of the difference $\hat{p}(Y = y_n | \mathbf{x}_n) - \mathbb{P}(Y = y_n | \mathbf{x}_n)$ in the estimated and true probabilities for the $K = 5$ categories across 20 simulated data sets with $N = 1000$ (left) and $N = 5000$ (right) data points for the survival functions in Figure 1 (top to bottom).

considered error measures $\text{MAE}(k)$ and MAE , and their variances, became smaller when the size of the data sets increased from 1000 to 5000. This, together with many additional numerical experiments we carried out, provides some empirical evidence of that the model and the estimation algorithm are working in the right way in the sense of $\hat{p}(k | \mathbf{x}_n)$ providing, for large data sets, consistent estimates of the true values $\mathbb{P}(k | \mathbf{x}_n)$. Moreover, Figure 3 shows that the differences between the estimated and true probabilities are approximately symmetrically distributed around 0 in the middle categories 2, 3 and 4; however, particularly in category 1 there appears to be some bias towards positive values. A closer examination of the covariate values with the largest differences between true and estimated values reveals that many of them are located close to the boundaries of the unit square, in particular, close to the origin $\mathbf{x} = (0, 0)$; see Figure S3 in the online Supplementary Material for the data points with the largest estimation errors.

The poor fit very close to the boundaries can be explained as follows: Suppose that (y_1, \mathbf{x}_1) is the observation with the smallest value for the first covariate x_1 . Then, the estimate maximizing the likelihood value for this observation would be $\hat{\lambda}_k(\mathbf{x}_1) = 0$ for $k > y_1$ and $\hat{\lambda}_k(\mathbf{x}_1) = 1$ for $k \leq y_1$. In case $y_1 = 1$, the likelihood function thus pushes the estimates towards $\hat{\lambda}_k(\mathbf{x}_1) = 0$ for all k , and as \mathbf{x}_1 has the smallest value for x_1 , there are no other data from which to draw inference. Consequently, the estimated functions will be close to 0 if $y_1 = 1$. If $y_1 \neq 1$, this is less problematic, because the effect of the data point (y_1, \mathbf{x}_1) favouring $\hat{\lambda}_2 = 1$ would be mitigated by the other data points. A similar argument can be made for values close to $x_1 = 1$ or $x_2 = 1$ and $y_t = K$. These difficulties are ameliorated to some extent when using the conditional prior proposed in Section 2.3.2 with the user-specified parameter d set to $d = K = 5$; a comparison of the posterior estimates for $\lambda_1, \dots, \lambda_5$ is provided in Section S1.4 of the online Supplementary Material.

3.2 Semi-parametric model structures

As in the non-parametric case, we consider three sets of functions for the semi-parametric model structure. The monotonic functions $\lambda_2, \dots, \lambda_5$ have the same shape as in Figure 1, but with the functional levels scaled to the interval $[-2, 2]$ instead of $[0, 1]$. These functions result in categories 1 and 5 being observed the most in all three studies; the proportions of observations in category 1 are 0.25, 0.39 and 0.25

Table 2: Error measures $\text{MAE}(k) \times 10^2$ and $\text{MAE} \times 10^2$, with standard deviations $\times 10^2$, computed from 20 sets of simulated data for the semi-parametric models in Section 3.2, for $N = 1000$ and $N = 5000$ data points.

Functions	N	MAE(1)	MAE(2)	MAE(3)	MAE(4)	MAE(5)	MAE
Linear	1000	3.7 (0.8)	2.0 (0.6)	1.8 (0.7)	1.8 (0.7)	3.3 (0.6)	3.6 (0.3)
	5000	2.1 (0.4)	1.2 (0.4)	1.1 (0.3)	1.0 (0.3)	2.2 (0.4)	2.2 (0.1)
Cont.	1000	4.7 (0.7)	2.3 (0.5)	2.0 (0.5)	2.3 (0.9)	3.1 (0.7)	4.2 (0.3)
	5000	3.2 (0.5)	1.5 (0.3)	1.4 (0.3)	1.4 (0.3)	2.0 (0.4)	2.6 (0.1)
Discont.	1000	4.2 (0.6)	3.8 (0.6)	4.2 (0.5)	4.7 (0.6)	3.9 (0.8)	4.6 (0.3)
	5000	2.7 (0.5)	2.3 (0.3)	2.1 (0.3)	2.4 (0.3)	2.3 (0.4)	2.5 (0.2)

for the set of linear, continuous and discontinuous functions respectively, while these proportions are 0.25, 0.27 and 0.34 for category 5. The vector $\boldsymbol{\beta}$ of linear regression coefficients in expression (3) is fixed to $\boldsymbol{\beta} = (\beta_1, \beta_2, \beta_3) = (0.3, -0.5, 0.1)$ and the covariates are independently and standard normally distributed, $\mathbf{z} \sim \text{MVN}(0, I_{3 \times 3})$, across all studies. This setup yields that the survival functions have shapes similar to those in Section 3.1, with the covariates \mathbf{z} having a moderate effect on the probabilities for the different categories; plots of the survival functions and an illustration of the effect of the values in \mathbf{z} are provided in Section S2.1 in the online Supplementary Material.

Table 2 shows again that the considered error measures $\text{MAE}(k)$ and MAE , and their variances, are decreasing with an increasing sample size. Moreover, the error measures are similar to the ones in Table 1. By plotting the posterior mean estimates, we find that the function estimates $\hat{\lambda}_2, \dots, \hat{\lambda}_5$ strongly resemble the true functions, and that the 95% central credibility intervals for $\hat{\boldsymbol{\beta}}$ include the true values in all but one repetition; posterior density plots for $\hat{\boldsymbol{\beta}}$ are shown in Figure S7 in the online supplementary material. As for the non-parametric case, the highest differences between the estimated and true probabilities, $\hat{p}(y_n | \mathbf{x}_n)$ and $\mathbb{P}(y_n | \mathbf{x}_n)$ ($n = 1, \dots, N$), occur for the first and last category; box plots of the difference are provided in Figure S8 in the online Supplementary Material. Based on this, our conclusion is that the proposed approach works well for both non-parametric and semi-parametric model structures.

4 Illustrations with real data

4.1 PISA schools data set

With our first real data example, we wanted to illustrate (i) the ability of the proposed approach to accommodate both continuous and ordered categorical covariates, (ii) the use of semi-parametric formulations allowing for cluster-level random effects as outlined in Section 2.2, and (iii) the graphical presentation of the model output in 3-dimensional surface plots. For this purpose, we analyzed data from the 2015 PISA school questionnaire (OECD, 2016), with responses from 14,491 schools in 67 countries. The outcome variable, measured in ordinal scale, was the agreement with the statement “In your school, to what extent is the learning of students hindered by the following phenomena? – Teachers not meeting individual students’ needs”. The question was answered by the principal/headteacher of the school, using the response categories “Not at all” (1), “Very little” (2), “To some extent” (3) or “A lot” (4). As independent variables, we included two measures for the size of the school, namely the average class size, recorded in categories 15 students or fewer, 16-20, 21-25, 26-30, 31-35, 36-40, 41-45, 46-50, more than 50 students, and the total enrolment, recorded as a count. We excluded 69 schools where the reported average class size conflicted with the enrolment, thus including 14,422 in the analysis.

For our analysis, we used the empirical cumulative distribution function (ECDF) transformation to scale the covariates to the interval $[0, 1]$, and then modeled their joint effect non-parametrically. The country effect was modeled with a logit link by including a zero mean normally distributed country-specific random effect into the linear predictor, with variance estimated from the data and updated in the MCMC algorithm from a conjugate inverse gamma posterior. The non-parametric regression surfaces were allowed to vary on logit scale in the interval $[-5, 5]$. The hyperparameters were chosen to be $a = 0.1$ and $b = 0.1$ for the Poisson point process intensities, with uniform priors for function levels ($d = 0$). The MCMC algorithm was run for 10,000 rounds after a 5,000 round burn-in, saving every 20th iteration. For a comparison, we also fitted a corresponding proportional odds mixed effects model, with additive linear effects for the two covariates on the logit scale (with total number of students entered into the model log transformed).

The model fit is illustrated in Figure 4a, showing a significant improvement over the proportional odds model. There was substantial country effect on the responses,

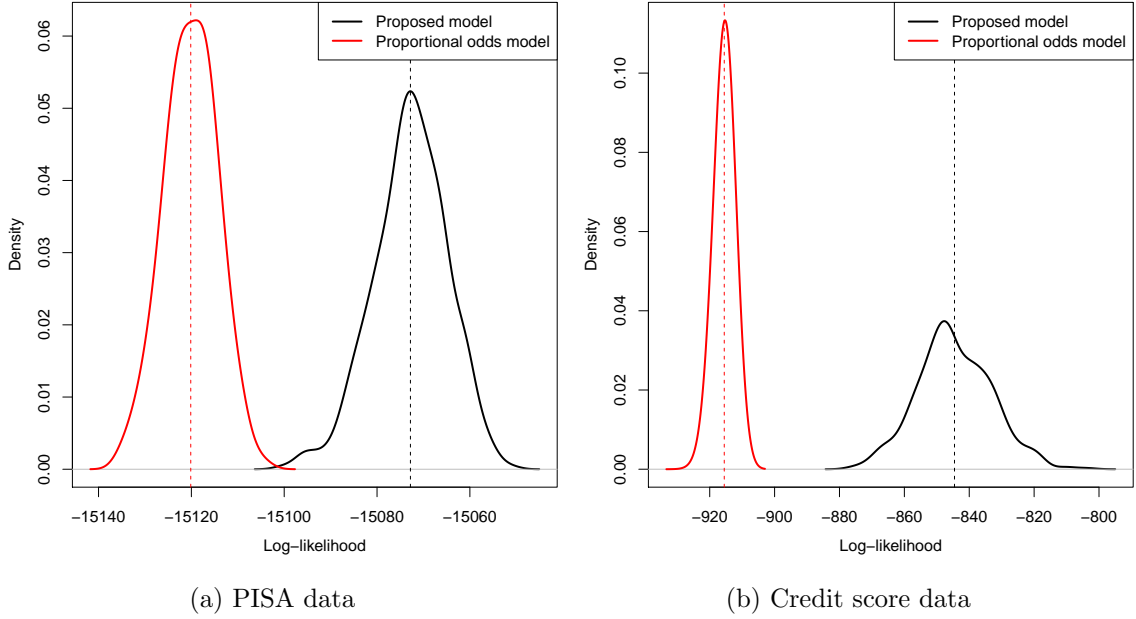


Figure 4: Panel (a): Density plot of the log-likelihood posterior distribution for the proposed model (blue lines) and the proportional odds model (red lines) fitted to PISA data. Panel (b): the same in the credit score data. The vertical dashed lines indicate posterior mean log-likelihood.

with the posterior median random effect variance of 0.53 and 90% credible interval (0.40, 0.73). The resulting posterior mean regression surfaces for the three cumulative response category probabilities are shown in the perspective plot of Figure 5. An alternative presentation where the layers are shown separately rather than overlaid, is provided in the Supplementary Materials. The posterior mean regression surfaces were calculated at fixed covariate values \mathbf{x} and cluster levels c as $\frac{1}{L} \sum_{\ell=1}^L S(k | \mathbf{x}, c; \lambda_k^{(\ell)})$, where $\lambda_k^{(\ell)}, \ell = 1, \dots, L$ is the posterior sample for the level k regression function. For Figure 5, the country effect was set to the expected value of zero, while the class size and school size were varied on a rectangular grid. The distribution of the data points on ground level shows the correlation between the two main covariates. Notable about the covariate effects is that the effect of the school size on the ‘not meeting the individual students’ needs’ response seems to level off, while the effect of the class size mainly seems to be present in relatively small schools. For comparison, Supplementary Materials include a similar perspective plot under the proportional odds model; the log-linearity assumption for school size on the link function scale produces an s-shaped surface for the predicted probabilities, which looks less reasonable in the boundaries

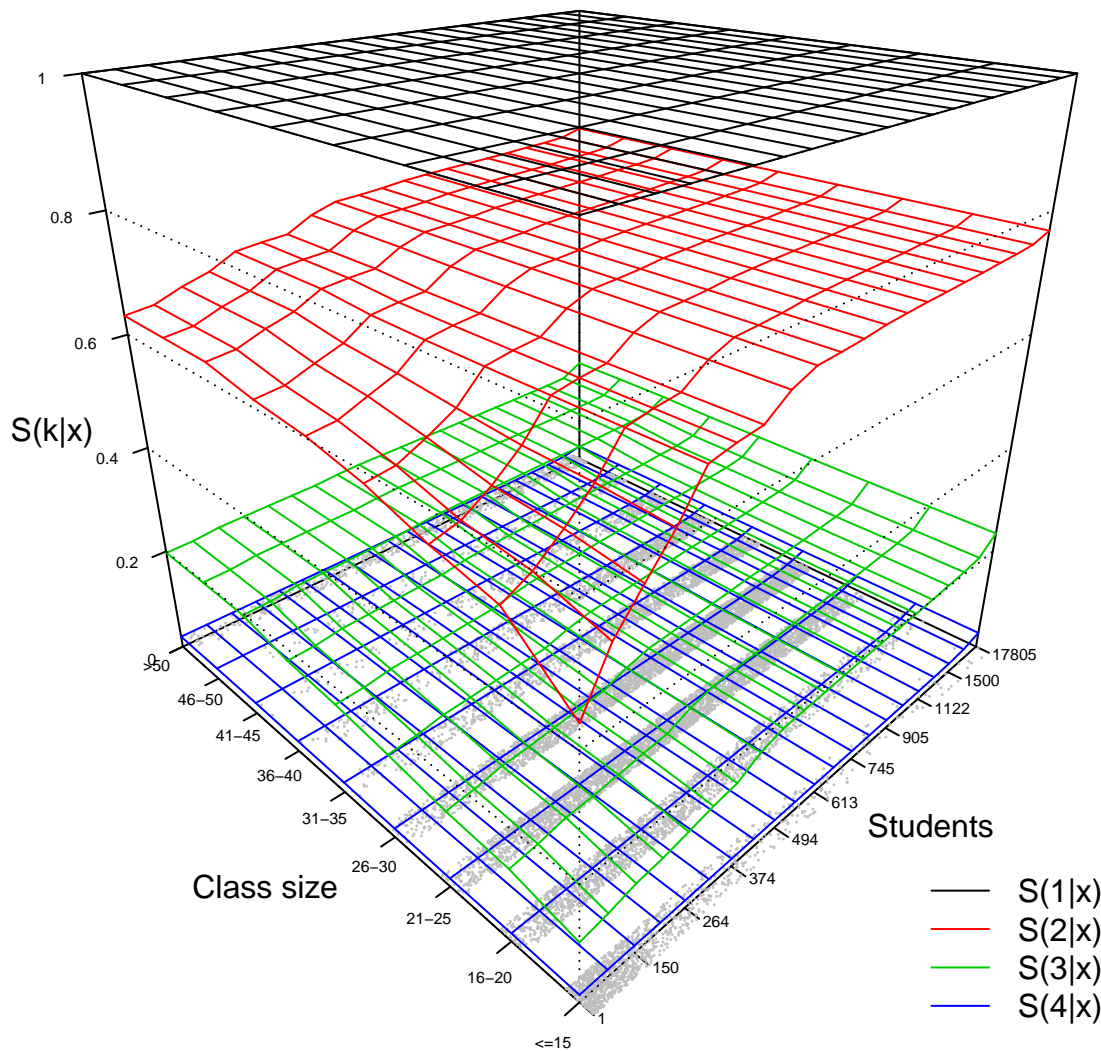


Figure 5: A perspective plot of the posterior mean regression surfaces for the three cumulative response category probabilities in the PISA data analysis. The jittered dots show the covariate coordinates of the data points.

of the data, explaining the worse fit in Figure 4a.

Another way to present the model results is shown in Figure 6, where the conditional posterior mean regression functions are presented as functions of class size at different values of school size. Here the posterior mean regression surfaces are shown for two countries, Great Britain (GBR) and Czech Republic (CZE), for which the 90% credible intervals for the country specific random effects were the first to not overlap with zero

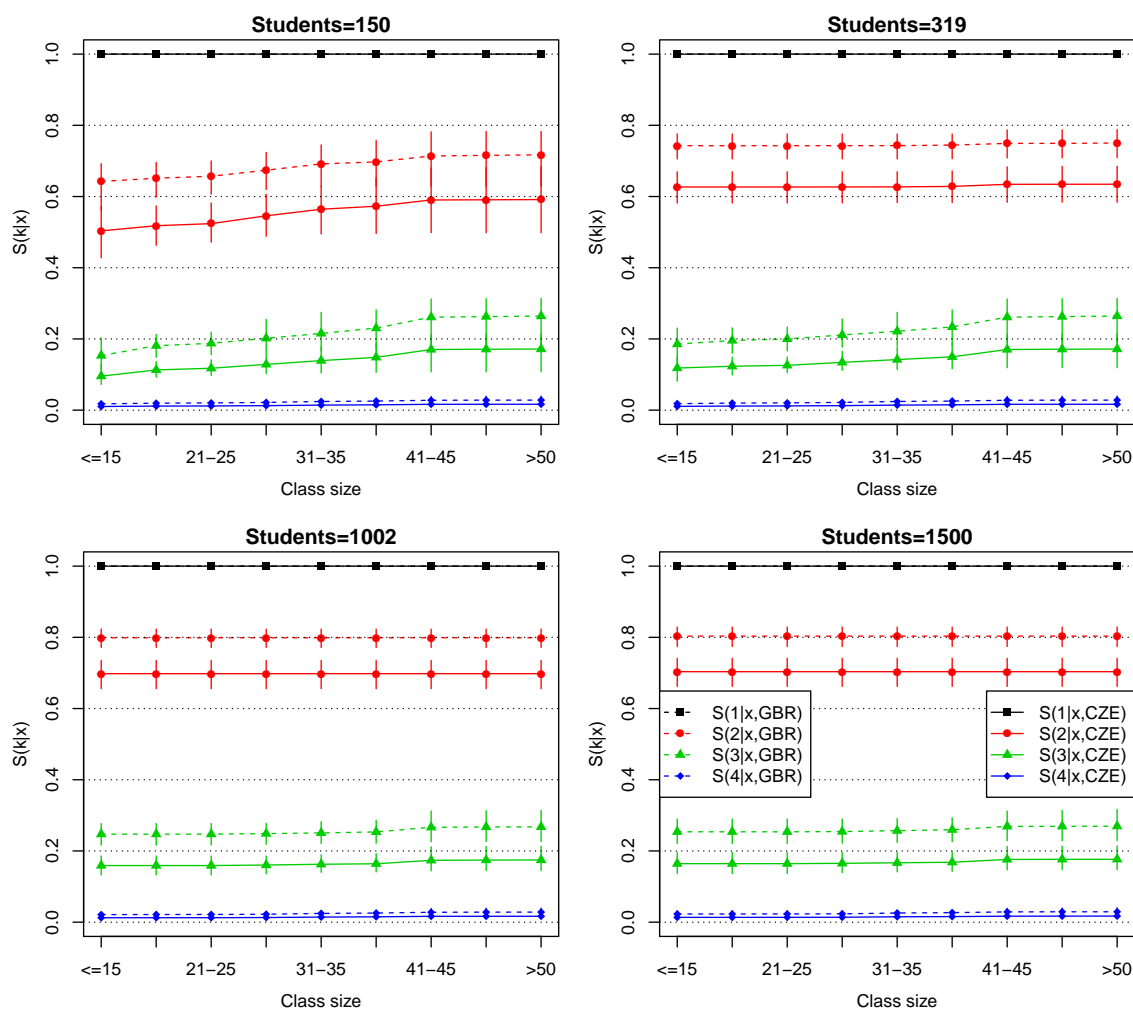


Figure 6: Conditional posterior mean regression functions for the three cumulative response category probabilities in the PISA data analysis, as functions of class size.

to the opposite directions (see the Supplementary Materials for all the country effects). The 90% credible intervals for the regression surfaces are mostly non-overlapping for these two countries, and the country effect seems comparatively larger than either of the covariate effects.

4.2 Credit score data set

In our second real data example, we wanted to demonstrate (i) the ability of the proposed method to incorporate multiple covariates, (ii) the workings of the inbuilt model selection functionality, and (iii) the graphical presentation of the results in a

higher dimensional setting. For this purpose, we reanalysed the credit score data set considered by DeYoreo and Kottas (2018). The response here was the 7-level credit rating of 921 US companies, re-coded into 5 categories by combining the two lowest and two highest ratings which were rare. The data set has five covariates, viz., book leverage (BOOKLEV), earnings before interest and taxes, divided by total assets (EBIT), log-sales (LOGSALES), retained earnings divided by total assets (RETA), and working capital divided by total assets (WKA). All of these were assumed to have a monotonically increasing effect on the cumulative credit rating probabilities, except BOOKLEV which was entered into the model as inverted. We modeled all five covariates non-parametrically, allowing the model to reduce to lower dimensions by defining all 31 point processes corresponding to the non-empty subsets of the covariates. We modeled the response with the logit link, allowing the surfaces to vary in the interval $[-10, 10]$, but with no additional parametric restrictions. Otherwise the priors were chosen as in the previous section. The covariates were re-scaled to the interval $[0, 1]$ using the ECDF transformation. The model fit was compared to a reference proportional odds model with additive and linear effects on the logit scale. The MCMC algorithm was run for 10,000 rounds after a 5,000 round burn-in, saving every 20th iteration.

Since in this context it might be of interest to consider each covariate's effect on the credit score while keeping the others constant, instead of the marginal regression functions, we present the results in terms of directly standardized regression functions for each covariate in turn, averaging over the empirical joint distributions of the other covariates as

$$\frac{1}{L} \sum_{\ell=1}^L \frac{1}{N} \sum_{n=1}^N \text{expit} \left(\lambda_k^{(\ell)}(x_{1n}, \dots, x_j = x, \dots, x_{pn}) \right)$$

for all $j, 1 \leq j \leq 5$. The resulting regression functions can then be presented as functions of x . Assuming that the distribution of the other covariates, viewed as confounders, remains constant, these functions can be given a causal interpretation as 'effects of x on the credit score'. Similarly, if multivariable effects are of interest, we can calculate regression surfaces on a grid of values (x, x') for covariates j and j' as

$$\frac{1}{L} \sum_{\ell=1}^L \frac{1}{N} \sum_{n=1}^N \text{expit} \left(\lambda_k^{(\ell)}(x_{1n}, \dots, x_j = x, \dots, x_{j'} = x', \dots, x_{pn}) \right)$$

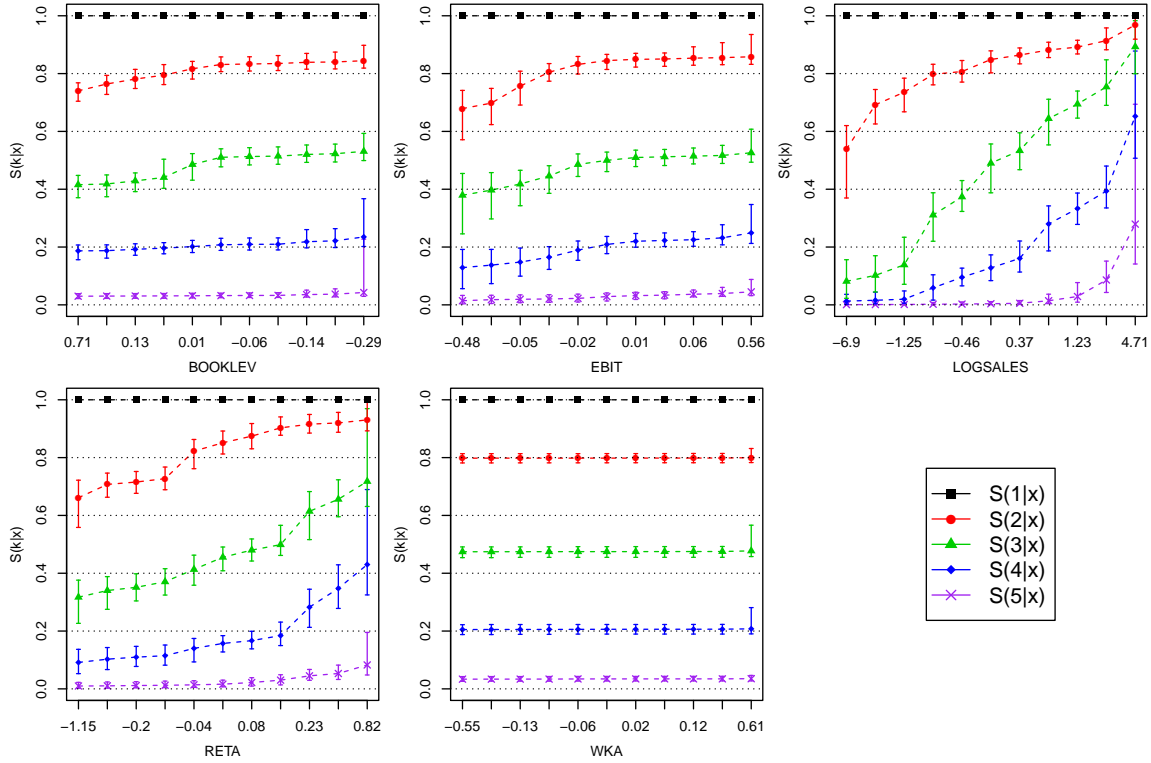


Figure 7: Standardized posterior mean regression functions for the four cumulative response category probabilities in the credit score data analysis, as functions of the different covariates.

and present these averaged over the posterior distribution λ_k in a 3-dimensional perspective plot. Because averaging over both the empirical distribution of the other covariates and the posterior distribution of the regression function realizations over a bivariate grid (x, x') potentially requires saving a very large number of predictions from the model, the order of averaging can be changed and the average over the posterior sample ℓ calculated as a rolling average over the MCMC run without saving multiple states of the chain.

The model fit comparison is presented in Figure 4b. We can again see a significant improvement over the proportional odds model, although there is considerable variability as the algorithm explores different model configurations. The standardized posterior regression functions are presented in Figure 7. The results correspond to those presented by DeYoreo and Kottas (2018) (although the standardized regression functions here are not directly comparable to the marginal regression functions presented therein), with LOGSALES and RETA being the strongest predictors, and

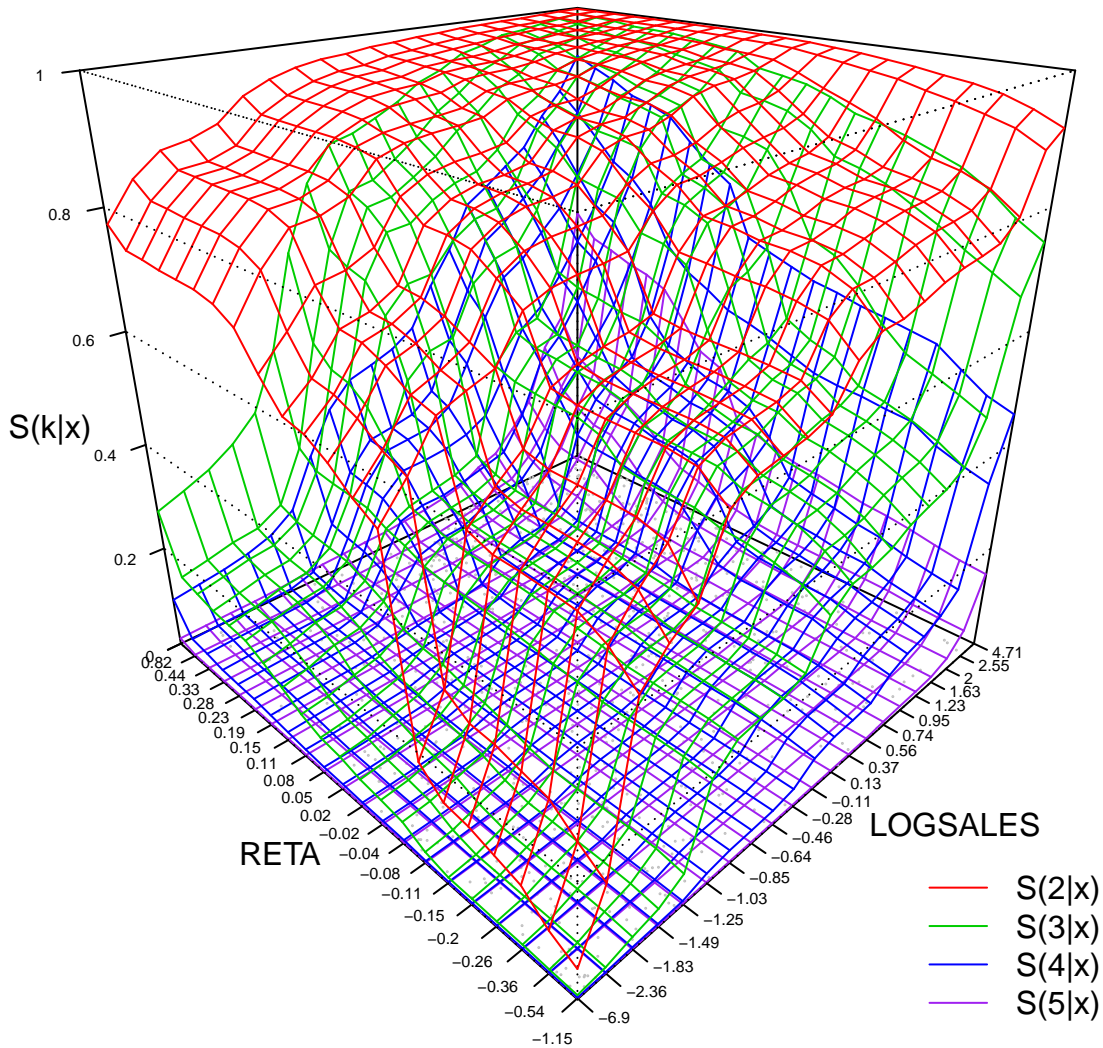


Figure 8: A perspective plot of standardized posterior mean regression surfaces for the four cumulative response category probabilities as functions of covariates RETA and LOGSALES in the credit score data. The dots show the covariate coordinates of the data points.

WKA the weakest. In fact, the algorithm often dropped the latter from the model altogether, leading to the flat regression function estimates. The probability of a covariate j being included in the model can be calculated from the MCMC run by taking the proportion of the iterations where $n(\Delta_i) > 0$ for at least one of the point processes defined in a subset of covariates involving j . These probabilities were 1

for all the other covariates but only 0.57 for WKA. Another measure of covariate selection would be the total count of random points in the configurations for the point processes defined in a subset of covariates involving j . The posterior means for these were 7.4 (BOOKLEV), 15.9 (EBIT), 27.2 (LOGSALES), 22.2 (RETA) and 1.1 (WKA). An example of 3-dimensional presentation of standardized regression surfaces as functions of LOGSALES and RETA is presented in Figure 8, demonstrating very strong association of the credit score with these two covariates, to the extent that some of the credit score levels are not present at all at certain combinations of these. An alternative presentation where the four layers are shown separately is presented in the Supplementary Materials.

5 Discussion

In this paper, we proposed a monotonic ordinal regression model and a Bayesian estimation procedure. The model differs from previous proposals in that it uses monotonicity as the only modeling assumption, without added proportionality, smoothness or distributional assumptions, while still enabling fully probabilistic inferences. Multivariable monotonicity of the covariate effects is a weaker assumption than the typically made additivity or linearity, although the present proposal does require specifying the direction of monotonicity a priori. Nevertheless, this assumption is often intuitively plausible on a priori basis, and our proposal extends multivariable monotonic regression to ordered categorical outcomes, replacing the common proportional odds assumption with monotonicity assumed for the cumulative probabilities of the ordered outcome categories. A general computational challenge in fitting non-proportional odds ordinal models is ensuring the ordering of the said cumulative probabilities; the present proposal resolves this naturally by combining the ordering constraints for monotonicity with ordering of the regression functions for the cumulative probabilities of the outcome categories.

As we demonstrated in our simulation study, the proposed model construction based on marked point processes is flexible and can approximate different continuous and non-continuous monotonic regression surfaces with increasing precision when the sample size increases. However, because the piecewise constant realizations we used to construct the regression surfaces are relatively inefficient in approximating smooth functions, requiring a large number of support points for good approximation,

the model may be best suited for large data sets. The advantage of the piecewise constant realizations is the ease of making local updating moves within the ordering constraints in the MCMC algorithm, but a disadvantage of lack of smoothness is the inability of the proposed model to extrapolate outside the support of the data. This may manifest as the “spiking” issue affecting traditional isotonic regression, giving unstable estimates near the boundaries of the data. Due to the asymmetric nature of the proposed construction, we observed this phenomenon mainly close to the origin, where the regression surface may not be supported from below by data points, allowing it to drop abruptly. To counter this, we suggested a conditional prior specification that can borrow strength from the regression surface levels above. Specifying continuous or smooth regression function realizations based on the marked point process construction is a topic for further research.

Due to the curse of dimensionality, it would be unrealistic to model the effects of a very large number of covariate non-parametrically. Because of this, we proposed a built-in model selection feature that allows dropping redundant covariates out from the model, as demonstrated in the application in Section 4.2. Also, we proposed a semi-parametric formulation that allows modeling the effects of the most important covariates non-parametrically, while simultaneously adjusting for a large number of other covariates. With this type of formulation, the proportional odds assumption could be tested by comparing models where a covariate is moved from the parametric to the non-parametric component through likelihood or Bayes factor.

To sum up, we have proposed a model and estimation method that is largely data driven, but may require a large sample size to produce accurate description of the regression surfaces. This is because, in the non-parametric ordinal regression problem, individual data points carry only relatively little information about each specific level of the ordered outcome. However, when large amounts of data are available, commonly made modeling assumptions such as linearity, additivity and proportional odds become restrictive, and the multivariable monotonicity assumption provides a more flexible alternative.

Code and data availability

The method will be made available as a function in the R package `monoreg` (Saarela, 2017) distributed through CRAN (<https://cran.r-project.org/>). The datasets

used for illustration are publicly available from OECD (<https://www.oecd.org/pisa/data/>) and from the Supplementary Materials to DeYoreo and Kottas (2018), available at <https://www.tandfonline.com/doi/suppl/10.1080/10618600.2017.1316280>.

Acknowledgement

The work of Olli Saarela was supported by a Discovery Grant from the Natural Sciences and Engineering Research Council of Canada. Christian Rohrbeck was beneficiary of an AXA Research Fund postdoctoral grant. The work of Elja Arjas was supported by the Big Insight research programme, University of Oslo. We are grateful to Arnaldo Frigessi for arranging for us a short visit at OCBE, during which some important steps were made towards completing this paper.

References

- Agresti, A. (2003). *Categorical Data Analysis*, volume 482. John Wiley & Sons.
- Agresti, A. (2010). *Analysis of Ordinal Categorical Data*, volume 656. John Wiley & Sons.
- Albert, J. H. and Chib, S. (1993). Bayesian analysis of binary and polychotomous response data. *Journal of the American Statistical Association*, 88(422):669–679.
- Ananth, C. V. and Kleinbaum, D. G. (1997). Regression models for ordinal responses: a review of methods and applications. *International Journal of Epidemiology*, 26(6):1323–1333.
- Ashby, D., Pocock, S. J., and Shaper, A. G. (1986). Ordered polytomous regression: an example relating serum biochemistry and haematology to alcohol consumption. *Journal of the Royal Statistical Society: Series C (Applied Statistics)*, 35(3):289–301.
- Bao, J. and Hanson, T. E. (2015). Bayesian nonparametric multivariate ordinal regression. *Canadian Journal of Statistics*, 43(3):337–357.
- Barlow, R. E. and Brunk, H. D. (1972). The isotonic regression problem and its dual. *Journal of the American Statistical Association*, 67(337):140–147.

- Bender, R. and Grouven, U. (1998). Using binary logistic regression models for ordinal data with non-proportional odds. *Journal of Clinical Epidemiology*, 51(10):809–816.
- Brant, R. (1990). Assessing proportionality in the proportional odds model for ordinal logistic regression. *Biometrics*, 46(4):1171–1178.
- Chib, S. and Greenberg, E. (2010). Additive cubic spline regression with Dirichlet process mixture errors. *Journal of Econometrics*, 156(2):322–336.
- Chipman, H. A., George, E. I., McCulloch, R. E., and Shively, T. S. (2016). High-dimensional nonparametric monotone function estimation using BART. *arXiv preprint arXiv:1612.01619*.
- Congdon, P. (2005). *Bayesian Models for Categorical Data*. John Wiley & Sons.
- DeYoreo, M. and Kottas, A. (2018). Bayesian nonparametric modeling for multivariate ordinal regression. *Journal of Computational and Graphical Statistics*, 27(1):71–84.
- Espinosa, J. and Hennig, C. (2019). A constrained regression model for an ordinal response with ordinal predictors. *Statistics and Computing*, 29(5):869–890.
- Green, P. J. (1995). Reversible jump Markov chain Monte Carlo computation and Bayesian model determination. *Biometrika*, 82(4):711–732.
- Gutierrez, P. A., Perez-Ortiz, M., Sanchez-Monedero, J., Fernandez-Navarro, F., and Hervás-Martínez, C. (2015). Ordinal regression methods: survey and experimental study. *IEEE Transactions on Knowledge and Data Engineering*, 28(1):127–146.
- Harrell Jr, F. E. (2015). *Regression modeling strategies: with applications to linear models, logistic and ordinal regression, and survival analysis*. Springer.
- Johnson, V. E. and Albert, J. H. (1999). *Ordinal Data Modeling*. Springer Science & Business Media.
- Kotłowski, W. and Slowinski, R. (2012). On nonparametric ordinal classification with monotonicity constraints. *IEEE Transactions on Knowledge and Data Engineering*, 25(11):2576–2589.

- Lall, R., Campbell, M., Walters, S., and Morgan, K. (2002). A review of ordinal regression models applied on health-related quality of life assessments. *Statistical Methods in Medical Research*, 11(1):49–67.
- Lehmann, E. L. (1966). Some concepts of dependence. *The Annals of Mathematical Statistics*, 37(5):1137–1153.
- Lin, L. and Dunson, D. B. (2014). Bayesian monotone regression using Gaussian process projection. *Biometrika*, 101(2):303–317.
- McCullagh, P. (1980). Regression models for ordinal data. *Journal of the Royal Statistical Society: Series B (Methodological)*, 42(2):109–127.
- McKinley, T. J., Morters, M., Wood, J. L., et al. (2015). Bayesian model choice in cumulative link ordinal regression models. *Bayesian Analysis*, 10(1):1–30.
- OECD (2016). *PISA 2015 Results (Volume I): Excellence and Equity in Education*. OECD Publishing, Paris.
- Peterson, B. and Harrell Jr, F. E. (1990). Partial proportional odds models for ordinal response variables. *Journal of the Royal Statistical Society: Series C (Applied Statistics)*, 39(2):205–217.
- R Core Team (2020). *R: A Language and Environment for Statistical Computing*. R Foundation for Statistical Computing, Vienna, Austria.
- Rohrbeck, C., Costain, D. A., and Frigessi, A. (2018). Bayesian spatial monotonic multiple regression. *Biometrika*, 105(3):691–707.
- Saarela, O. (2017). *monoreg: Bayesian Monotonic Regression Using a Marked Point Process Construction*. R package version 1.2.
- Saarela, O. and Arjas, E. (2011). A method for Bayesian monotonic multiple regression. *Scandinavian Journal of Statistics*, 38(3):499–513.
- Stout, Q. F. (2015). Isotonic regression for multiple independent variables. *Algorithmica*, 71(2):450–470.

Tutz, G. and Scholz, T. (2003). Ordinal regression modelling between proportional odds and non-proportional odds. Technical Report, Institute of Statistics, University of Munich.

Wu, J., Meyer, M. C., and Opsomer, J. D. (2015). Penalized isotonic regression. *Journal of Statistical Planning and Inference*, 161:12–24.